Interrogation of N-Linked Oligosaccharides Using Infrared Multiphoton Dissociation in FT-ICR Mass Spectrometry

Katherine S. Lancaster, Hyun Joo An, Bensheng Li, and Carlito B. Lebrilla*

Department of Chemistry, Department of Biochemistry— School of Medicine, University of California, Davis, Davis, California 95616

The structural elucidation of oligosaccharides remains a major challenge. Mass spectrometry provides a rapid and convenient method for structural elucidation based on tandem mass spectrometry. Ions commonly are selected and subjected to collision-induced dissociation (CID) to obtain structural information. Unfortunately, N-linked oligosaccharides are relatively large compounds and are not readily fragmented using CID. In this report, we illustrate the use of infrared multiphoton dissociation (IRMPD) to obtain structural information for large N-linked oligosaccharides. The IRMPD and CID behavior of oligosaccharides were compared for high-mannose-type oligosaccharides. Fragmentation that could not be obtained through conventional CID in Fourier transform ion cyclotron resonance mass spectrometry was observed with N-linked oligosaccharides. O-Linked and N-linked glycans of similarly large sizes were compared. It was found that internal cross-ring cleavages were observed only for N-linked oligosaccharides. The mannose branch points of N-linked oligosaccharides are apparently more susceptible to cross-ring cleavages.

Glycosylation is a common posttranslational modification of proteins whereby glycans are added to the protein chain. These glycans or oligosaccharides play many important biological roles.[1] It has been shown, for example, that removal of the oligosaccharides often prevents complete or even correct protein folding.[2−4] Glycans play a role in immunity[5] and fertilization,[6−8] and may provide important biological markers for a wide variety of diseases.[5,9,10] The complete structures of oligosaccharides are often difficult to obtain. Unlike proteins, the primary structures of oligosaccharides are often not linear, and multiple branches are

common. Furthermore, the structure of oligosaccharides cannot be predicted from genomic data, as with proteins. This complexity is due to the competitive nature of glycosyltransferases and glycosidases that produce oligosaccharides.[11] The common neutral monosaccharides found in humans have five attachment sites, with each attachment potential having two anomeric characters. Combined, these variations lead to a large number of possible structures.

Structural elucidation in mass spectrometry primarily employs collision-induced dissociation (CID).[12−14] This process involves first isolating the ion of interest from the complex mixture of ions generated during the ionization event. The ion is translationally excited and collided with an inert gas. Kinetic energy from the collision is converted into internal energy, which leads to bond-breaking reactions. The resulting fragments are observed in a tandem mass spectrum (MS/MS). In Fourier transform ion cyclotron resonance mass spectrometry (FT-ICR MS) there are some drawbacks to the use of CID. The common translational excitation event for CID in FT-ICR MS is sustained off-resonance irradiation (SORI).[15] During this excitation event, energy is provided to the ion at a frequency slightly off-resonance from the cyclotron frequency of the ion. This causes the ion to cycle in and out of the center of the ion cyclotron resonance (ICR) cell, gaining a small amount of internal energy with each collision. Optimization of this event is time-consuming because electrode voltages, frequency, and irradiation time must all be controlled for effective fragmentation. Furthermore, in FTMS, it is also imperative that the collision gas should be removed from the ICR cell prior to detection.

CID is notoriously inefficient in fragmenting large ions.[16,17] Larger ions commonly require multiple CID events for complete fragmentation and structural determination. Each isolation/

(1) Varki, A. *Glycobiology* **1993**, *3*, 97−130.
(2) Gallagher, P.; Henneberry, J.; Wilson, I.; Sambrook, J.; Gething, M.-J. *J. Cell Biol.* **1988**, *107*, 2059−2073.
(3) Dube, S.; Fisher, J. W.; Powell, J. S. *J. Biol. Chem.* **1988**, *263*, 17516−17521.
(4) Parodi, A. J. *Ann. Rev. Biochem.* **2000**, *69*, 69−93.
(5) Rudd, P. M.; Elliott, T.; Cresswell, P.; Wilson, I.; Dwek, R. A. *Science* **2001**, *291*, 2370−2376.
(6) Zhang, J.; Xie, Y.; Hedrick, J.; CB, L. *Anal. Biochem.* **2004**, *334*, 20−35.
(7) Yonezawa, N.; Amari, S.; Takahashi, K.; Imai, F. L.; Kanai, S.; Kikuchi, K.; Nakano, M. *Mol. Reprod. Dev.* **2005**, *70*, 222−227.
(8) Takemoto, T.; Natsuka, S.; Nakakita, S.-i.; Hase, S. *Glycoconjugate J.* **2005**, *22*, 21−26.
(9) Parekh, R. B.; Dwek, R. A.; Sutton, B. J.; Fernandes, D. L.; Leung, A.; Stanworth, D.; Rademacher, T. W.; Mizuochi, T.; Taniguchi, T.; Matsuta, K.; Takeuchi, F.; Nagano, Y.; Miyamoto, T.; Kobata, A. *Nature* **1985**, *316*, 452−457.
(10) Juhasz, P.; Costello, C. E. *J. Am. Soc. Mass Spectrom.* **1992**, *3*, 785−796.
(11) Trombetta, E. S. *Glycobiology* **2003**, *13*, 77R−91R.
(12) Tseng, K.; Romero, A.; Hedrick, J.; Lebrilla, C. *Glycobiology* **1999**, *9*, 1153.
(13) Harvey, D. J. *J. Mass Spectrom.* **2000**, *35*, 1178−1190.
(14) Dell, A.; Morris, H. R. *Science* **2001**, *291*, 2351−2356.
(15) Gauthier, J. W.; Trautman, T. R.; Jacobson, D. B. *Anal. Chim. Acta* **1991**, *246*, 211−225.
(16) Biemann, K.; Martin, S. A. *Mass Spectrom. Rev.* **1987**, *6*, 1−76.
(17) Hunt, D. F.; Yates, J. R., III; Shabanowitz, J.; Winston, S.; Hauer, C. R. *Proc. Natl. Acad. Sci. U.S.A.* **1986**, *83*, 6233−6237.

fragmentation event causes ion loss, and a decrease in signal is inevitable. N-Linked oligosaccharides, with their highly branched core structures, have high masses and require multiple isolation/fragmentation events for complete structural elucidation. In FT-ICR MS, this makes the structural determination of N-linked oligosaccharides with CID difficult.

An MS/MS technique that rectifies many of the difficulties with CID is infrared multiphoton dissociation (IRMPD).[18,19] IRMPD allows for fragment ions that are generally similar to those observed in CID but without the difficulties that are associated with CID.[20-22] Unlike CID, IRMPD does not require a collision gas or for the ions to be translationally excited. IRMPD has also been shown to be much more efficient at fragmenting larger ions than CID;[21] therefore, it is predicted that the fragmentation of N-linked oligosaccharides is more accessible with IRMPD than CID.

In IRMPD, an ion of interest is isolated, but without the subsequent translational excitation, the ion remains in the center of the ICR cell, where it is irradiated with an infrared (IR) laser beam. As the ion absorbs the energy of the IR laser, the ion becomes vibrationally excited, causing bond breakage. The length of the irradiation event determines the number of photons absorbed and, thus, the amount of vibrational energy gained by the ions. The fragment ions are not removed from the center of the ICR cell and remain in the path of the laser. Therefore, they absorb energy and subsequently fragment then by removing the necessity for multiple isolation/fragmentation events. In CID, energy is deposited primarily in the precursor ions, and fragments do not further dissociate. It is easier to control the amount of energy being imparted to the ion with IRMPD, which is performed by adjusting the power of the laser and the length of irradiation.

In this report, we illustrate the application of IRMPD to large oligosaccharides that do not fragment completely under CID conditions. We have previously shown that O-linked oligosaccharides fragment readily under IRMPD conditions;[23] however, the structures of N-linked oligosaccharides are significantly enough different from O-linked oligosaccharides that they require their own investigation. The study demonstrates that CID and IRMPD provide similar fragment ions for N-linked oligosaccharides, but with a significantly better signal-to-noise ratio and more extensive fragmentation found in IRMPD.

EXPERIMENTAL SECTION

Methods and Materials. Ribonuclease B, chicken ovalbumin, and bovine fetuin were purchased from Sigma-Aldrich (St. Louis, MO) and used without further purification. Peptide-N-glycosidase F (PNGase F) was obtained from Calbiochem (La Jolla, CA). All solvents were of HPLC grade. The graphitized carbon cartridge (GCC) used for desalting was purchased from Alltech Associated,

Inc. (Deerfield, IL). Evaporation of small amounts of solvent was performed on a Centrivap Concentrator (Labconco Corp, Kansas City, MO).

Preparation of N-Linked Oligosaccharides. All N-linked oligosaccharides were released by incubating the glycoproteins with PNGase F (1 U) in 100 mM NH_4HCO_3 (pH 7.5) for 12 h at 37 °C. Placing the reaction vial in boiling water for 5 min halted the reaction.

Preparation of O-Linked Oligosaccharides. *Xenopus borealis* egg jelly was obtained, and the glycoprotein was purified as described in previous papers.[6,24] The glycans were released through a reductive β-elimination as previously described.[25]

Purification and Fractionation of Oligosaccharides Using Solid-Phase Extraction. Released oligosaccharides were purified using GCC. For each sample, a cartridge was washed with H_2O, followed by 0.1% (v/v) trifluoroacetic acid (TFA) in 80% acetonitrile (AcN)/H_2O (v/v). The solution containing the oligosaccharide was placed in the cartridge and loaded slowly. The cartridge sample was then washed with deionized water at a flow rate of ~1 mL/min to remove salts. The glycans were eluted with 10, 20, and 40% AcN with 0.05% TFA in H_2O, successively. Each fraction was collected and dried down prior to analysis with mass spectrometry.

Methylation of Sialyated Oligosaccharides. The sialyated oligosaccharides released from bovine fetuin were first dried by speed-vacuum centrifugation and reconstituted with 10 μL methyl iodide and 50 μL of anhydrous dimethyl sulfoxide.[26] The suspension was thoroughly mixed with vortexing and allowed to react for 2 h at room temperature. Solvent was subsequently removed by lyophilization. The methylated glycans were reconstituted in water prior to MALDI-FT-ICR MS analysis.

Mass Spectrometric Analysis. All mass spectra were obtained with an external source MALDI-FT-ICR mass spectrometer (HiRes MALDI, IonSpec Corp, Lake Forest, CA) equipped with a 7.0-T superconducting magnet. This instrument is equipped with a pulsed Nd:YAG laser (355 nm). A matrix of 2, 5-dihydroxybenzoic acid at a concentration of 0.1 M in 50:50 AcN/H_2O was used. To ensure the sodiated ion would be observed, the sample was doped with 0.1 M NaCl in 50:50 AcN/H_2O during MALDI spotting. The sample (1 μL) was spotted on a MALDI target plate, followed by the NaCl dopant (0.5 μL) and matrix (1 μL). The sample was allowed to dry in the air prior to analysis.

Collision Induced Dissociation. SORI-CID was performed by isolating the desired ion in the ICR cell using an arbitrary waveform generator. The ions were excited at 1000 Hz higher than their cyclotron frequency for 1000 ms at 2−8 V (base to peak), depending on desired level of fragmentation and the size of the oligosaccharide. Two argon pulses were used during the CID event to maintain a pressure of 10^{-5} Torr.

Infrared Multiphoton Dissociation. An infrared laser (Parallax Technology, Inc., Waltham, MA) was used to irradiate the ICR cell through a BaF_2 window. A tandem MS event began with the isolation of the ion using the arbitrary waveform generator. The ion was subsequently irradiated with an IR laser pulse lasting

(18) Novak, P.; Haskins, W. E.; Ayson, M., J.; Jacobsen, R. B.; Schoeniger, J. S.; Laeavell, M. D.; Young, M. M.; Kruppa, G. H. *Anal. Chem.* **2005**, *77*, 5101−5106.

(19) Woodin, R. L.; Bomse, D. S.; Beauchamp, J. L. *J. Am. Chem. Soc.* **1978**, *100*, 3248−3250.

(20) Zhang, J.; Schubothe, K.; Li, B.; Russell, S.; CB, L. *Anal. Chem.* **2005**, *77*, 208−214.

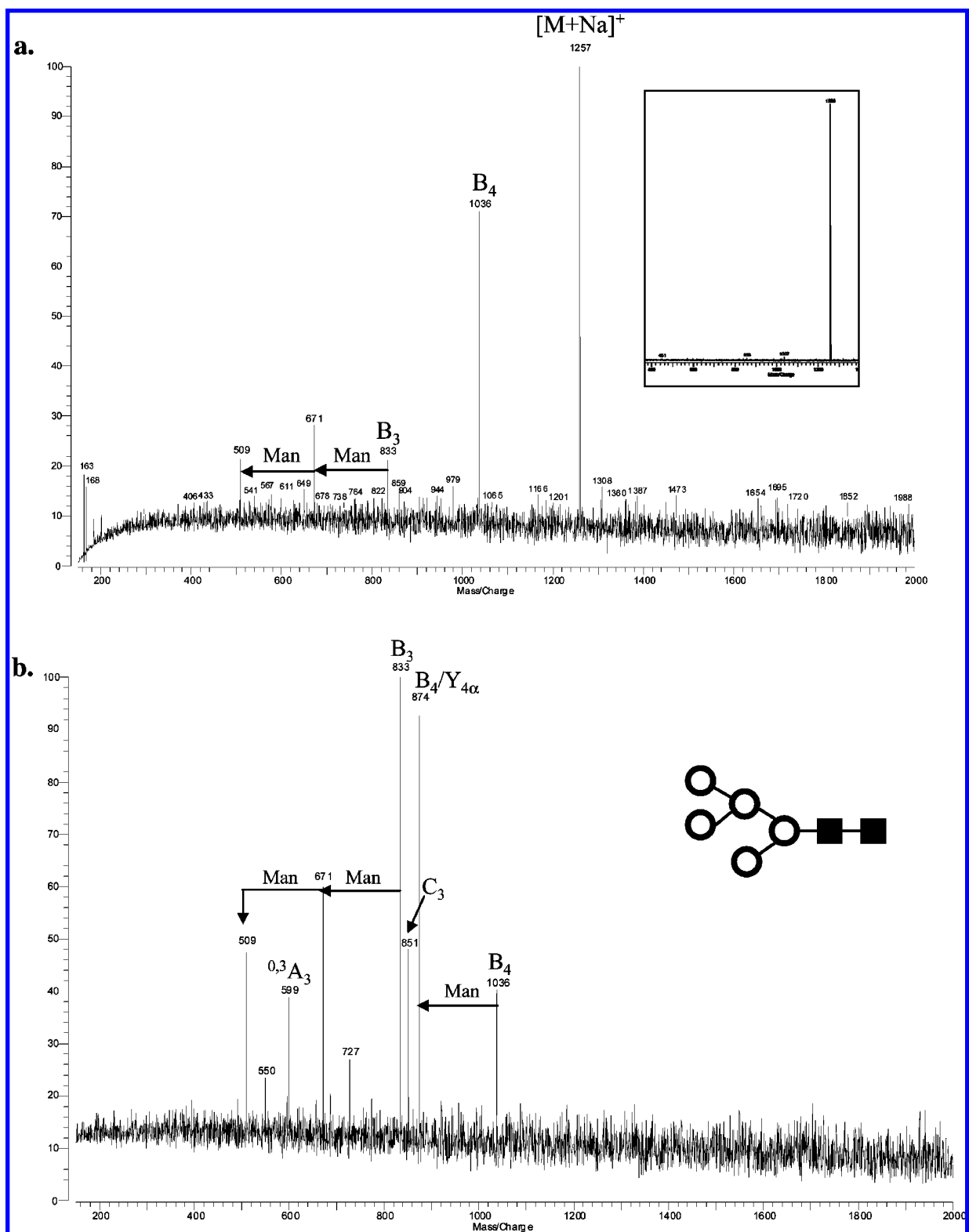(21) Xie, Y.; Lebrilla, C. *Anal. Chem.* **2003**, *75*, 1590−1598.

(22) Xie, Y.; Schubothe, K.; Lebrilla, C. *Anal. Chem.* **2003**, *75*, 160−164.

(23) Zhang, J. H.; Schubothe, K.; Li, B. S.; Russell, S.; Lebrilla, C. B. *Anal. Chem.* **2005**, *77*, 208−214.

(24) Zhang, J.; Lindsay, L.; Hedrick, J.; Lebrilla, C. B. *Anal. Chem.* **2004**, *76*, 5990−6001.

(25) Tseng, K.; Lindsay, L.; Penn, S.; Hedrick, J.; Lebrilla, C. *Anal. Biochem.* **1997**, *250*, 18−28.

(26) An, H. J.; Lebrilla, C. B. *Isr. J. Chem.* **2001**, *41*, 117−127.

Figure 1. (a) Collision-induced dissociation spectrum of Man 5. The isolated ion is sodiated with a m/z of 1257. Incomplete fragmentation was obtained. The inset shows the isolation of the quasimolecular ion prior to fragmentation. (b) MS/MS/MS (1257/1036) of the m/z 1036 ion with prior isolation. The inset shows the structure of Man 5. The filled squares represent GlcNAc, and the open circles represent mannose.

between 500 and 2000 ms. Laser power was measured at 14 W for all experiments described.

RESULTS

High-Mannose N-Linked Oligosaccharides. To compare the efficiencies of fragmentation for N-linked oligosaccharides,

the CID and IRMPD spectra were compared for two high-mannose-type N-linked oligosaccharides. Collision-induced dissociation (CID) of the high-mannose glycan $GlcNAc_2Man_5$ (Man 5) released from ribonuclease B did not readily produce fragments, resulting in a spectrum with a poor signal-to-noise ratio (Figure 1), despite the strong signal upon isolation (inset Figure
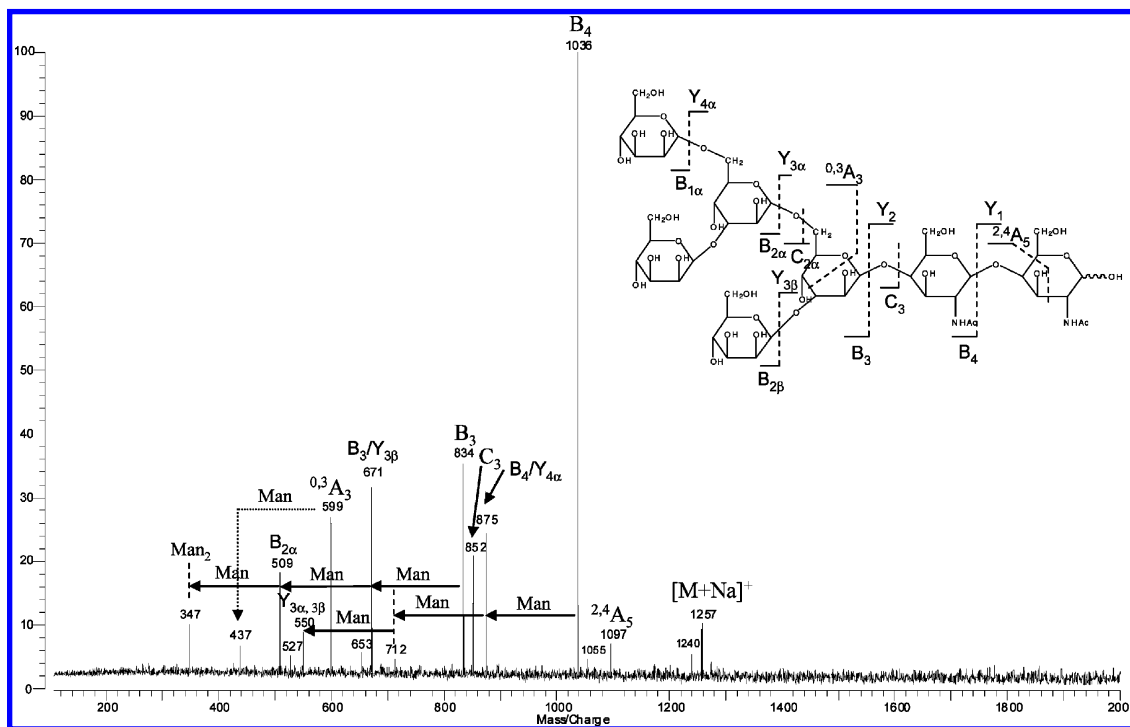
Figure 2. Infrared multiphoton dissociation spectrum of Man 5 (m/z 1257). The inset shows the structure with the observed fragmentations labeled. Cross-ring cleavages are observed at one of the core mannoses.
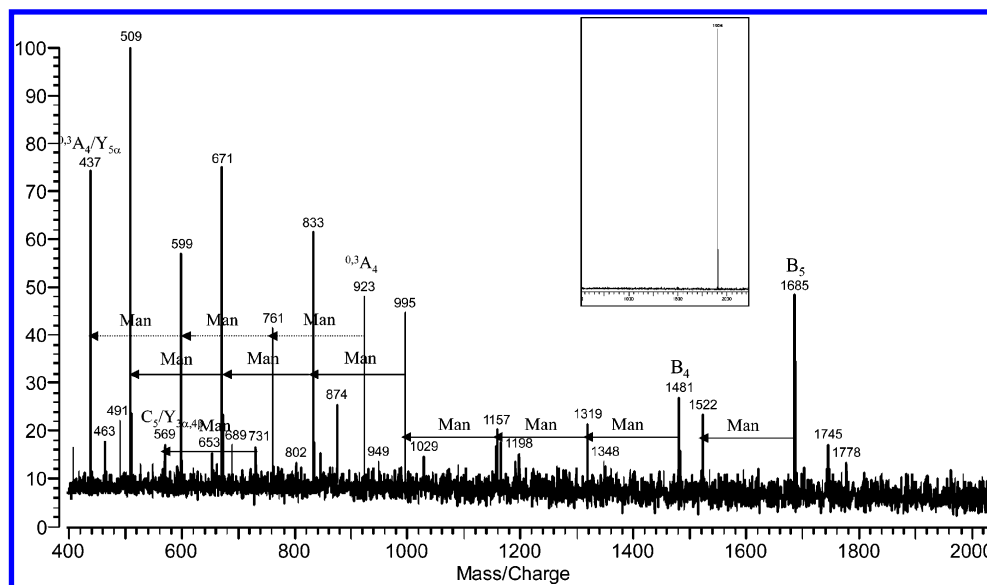

Figure 3. The collision-induced dissociation spectrum of Man 9 with isolation (inset). Glycosidic bond and some cross-ring cleavages are observed. See Figure 4 for the structure.

1a). The first MS/MS event did not completely fragment the quasimolecular ion (Figure 1a). In the spectrum, the parent ion has the highest intensity, with the primary fragment ion belonging to the loss of a GlcNAc, m/z 1036, to yield the B_4 fragment (Domon and Costello nomenclature).[27] In each case, the mass accuracy was significantly higher than that reported (10 ppm); however, only nominal masses are provided for clarity. A B_3 fragment is also observed with minor peaks corresponding to the losses of mannoses. To gain more structural information, the B_4 fragment was isolated and subjected to further CID analysis (MS³) (Figure 1b). The peaks observed were again primarily the B_3 ion

and the subsequent losses of mannose residues. A C_3 ion was observed, as well as one cross-ring cleavage product, $^{0,3}A_3$.

The infrared multiphoton dissociation spectrum of Man 5 is shown in Figure 2. This spectrum demonstrates the benefit provided by IRMPD where the fragment ions remain in the path of the IR beam. Further degradation of the fragments yielded structural information that required several stages of tandem MS to obtain with CID. This capability provides better signal-to-noise and more structural information from a single MS/MS event. The sodiated parent ion is observed at m/z 1257. Several peaks are

(27) Domon, B.; Costello, C. E. *Glycoconjugate* **1988**, *5*, 397−409.
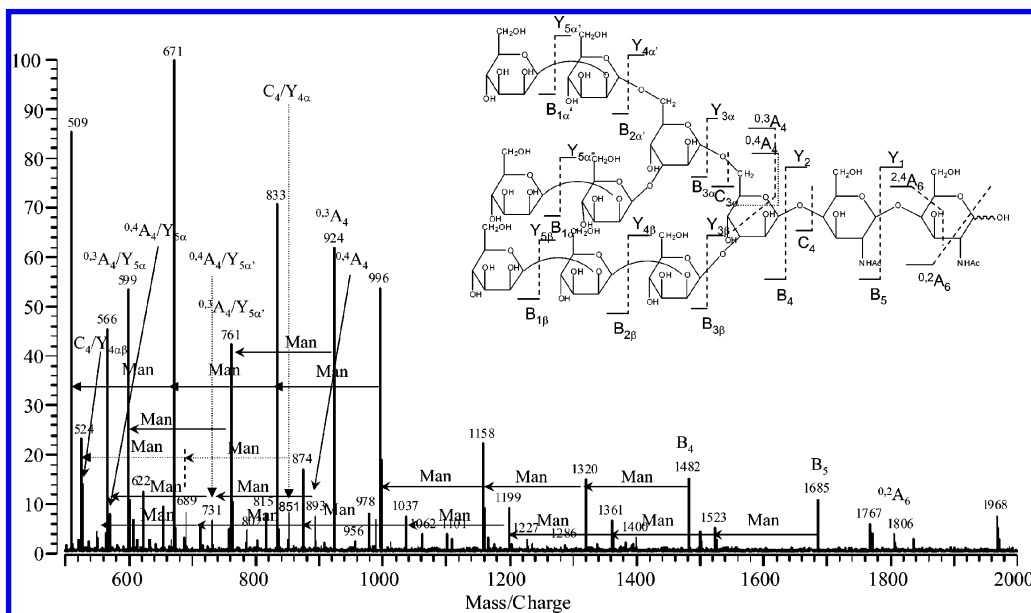
Figure 4. Infrared multiphoton dissociation spectrum of Man 9. The spectrum shows cross-ring cleavages with some branching information as well as B and Y fragments. The inset shows the structure of Man 9 with labeled fragmentations.
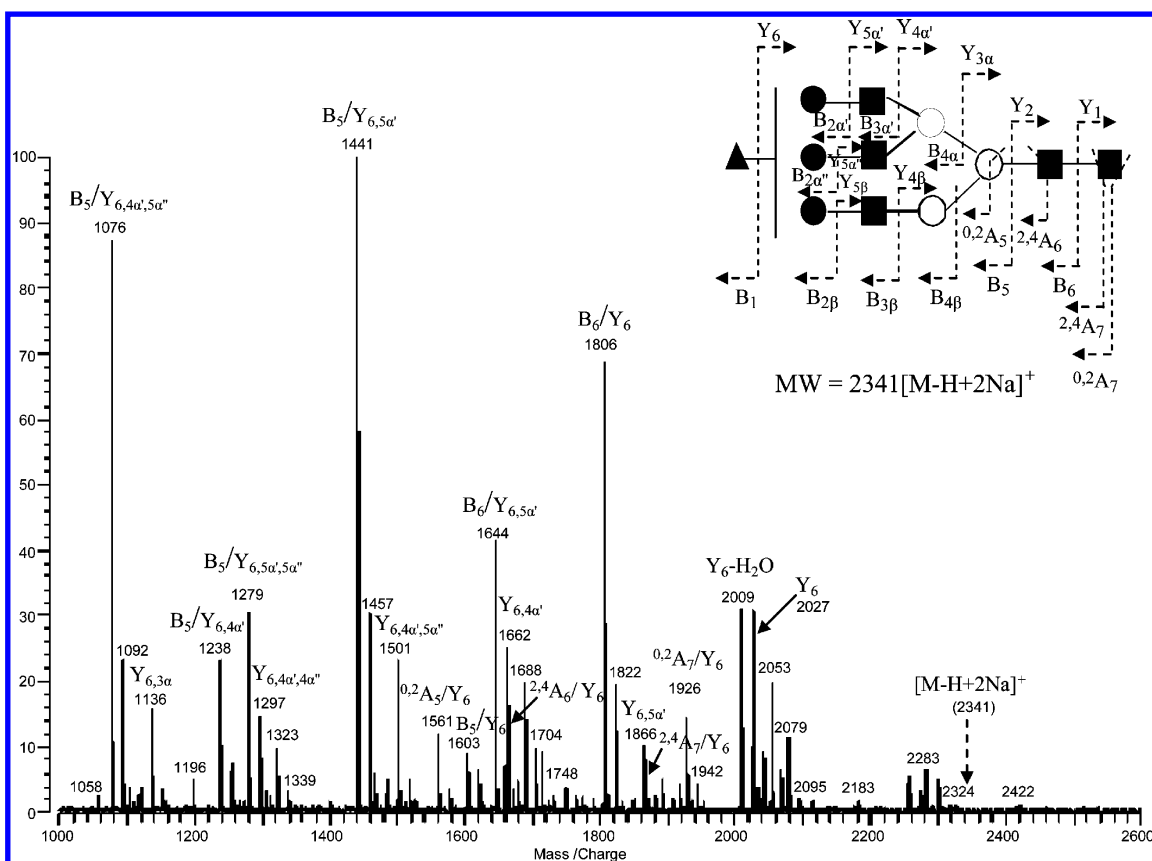

Figure 5. IRMPD spectrum of a monosialylated native glycan (m/z 2341) from bovine fetuin. The structure shows all the cleavages observed. Primarily B and Y ions were observed.

observed to aid in determination of the core structure of this N-linked oligosaccharide, including $^{2,4}A_5$ (m/z 1097) and $^{0,3}A_3$ (m/z 599). These ions are due to cross-ring cleavages. Several fragment ions corresponded to B, C, and Y ions and contained the GlcNAc residue of the core. The $^{0,3}A_3$ fragment from the branching mannose of the core aided in determination of the positions of the antennae. The B_4 and B_3 ions are observed as in the CID

spectrum (Figure 1), but other combinations, including fragments of these ions, are also observed (Figure 2). A useful fragment that is absent in the CID is the loss of mannose from the $^{0,3}A_3$ fragment, which identifies this fragment as belonging to the core mannose.

A larger high-mannose-type N-linked glycan with four additional mannoses, GlcNAc$_2$Man$_9$ (Man 9), was obtained from
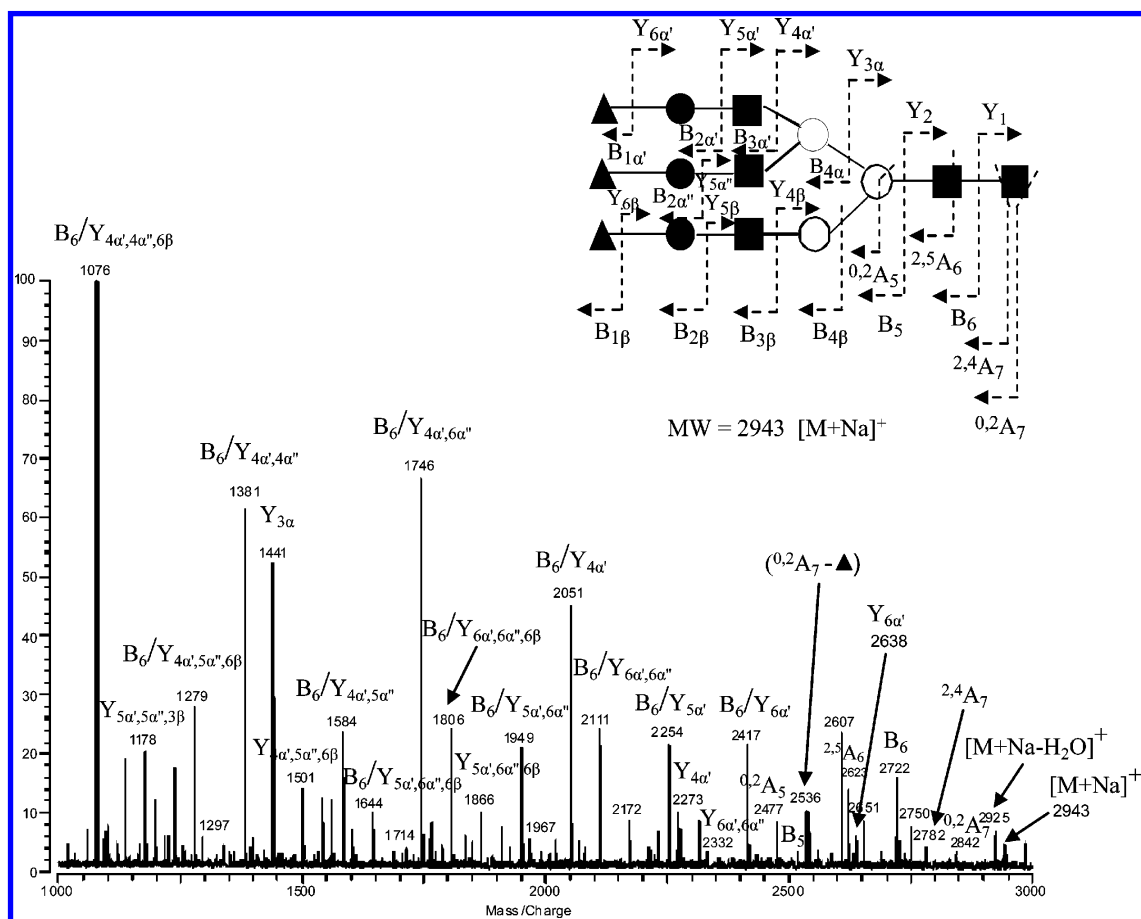
Figure 6. IRMPD spectrum of a trisialylated glycan from bovine fetuin. The sialic acids were methyl-esterified to produce the quasimolecular ion. The observed fragments with structure are labeled. The filled triangles (▲) represent the methylated sialic acid.

ribonuclease B and examined. Extensive fragmentation was observed for the CID of Man 9 (Figure 3). Interestingly, this ion did not require multiple fragmentation events. The resulting spectrum showed poor signal-to-noise, which is often observed in the CID spectra of large-mass oligosaccharides. The parent ion was isolated cleanly (inset Figure 3) and was not observed in this CID spectrum. Large ions were obtained corresponding to the B_5 and B_4 fragments (m/z 1685 and 1481, respectively). Subsequent mannose losses were clearly discernible (i.e., m/z 1481, 1319, 1157, and 995). No C fragments were observed; however, cross-ring cleavages were present. These ions originated from the cleavage of the branching mannose and corresponded to mannose losses from the $^{0,3}A_4$ fragment (m/z 923). A minor fragment corresponding to $^{0,4}A_4/Y_{5\alpha}$ was also observed (m/z 731) with an accompanying mannose loss (m/z 569). The cross-ring cleavages were limited and provided some information regarding the first branched residue and the positions of the antennae.

The IRMPD spectrum of Man 9 (Figure 4) showed significantly more structural information and a better signal-to-noise ratio. The sodiated parent ion was significantly decreased in this spectrum. A cross-ring cleavage of the reducing end, $^{0,2}A_6$, was the largest peak detected that was unique to IRMPD (m/z 1806). The B_5 and B_4 ions (m/z 1685 and 1482, respectively) were readily observed along with fragments corresponding to subsequent mannose losses. The extensive fragmentation represents a major difference between the CID and IRMPD spectra. The mannose losses from the B_5 ion were absent in the CID spectrum (Figure 3), whereas

both B_4 and B_5 showed prolific mannose losses in the IRMPD spectrum. The results demonstrate that with IRMPD, essentially every glycosidic bond cleavage is represented, and ion loss is minimized.

Another ion that was not observed in the CID spectrum is the C_4 fragment and subsequent losses of mannoses from this ion (C_4/Y_n). These ions were present at m/z 851, 689, and 527. They also corresponded to internal cleavages that were not represented in the CID spectrum. Other internal cleavages present in the IRMPD spectrum but not in the CID spectrum were several peaks that represent the cross-ring cleavages from the core branching mannose. These fragments were present at m/z 893, 731, and 569. They corresponded to the $^{0,4}A_4$ fragment with subsequent mannose losses. Another series representing the $^{0,3}A_4$ fragment and subsequent mannose losses (m/z 923, 761 and 599) were observed and more intense than the $^{0,4}A_4$ series. The information obtained in the IRMPD spectrum yielded more structural information for $GlcNAc_2Man_9$ than was possible for CID.

Complex-Type N-Linked Oligosaccharides. Oligosaccharides with labile moieties, such as sialic acids, are difficult to analyze with MALDI. Sialylation often accompanies complex oligosaccharides; however, producing the molecular ions is complicated by the loss of the sialic acid, particularly for those containing more than one sialic acid residue. To preserve the molecular ion, methyl esterification is commonly used. To determine whether IRMPD could be used to determine the position of the sialic acid, complex N-linked oligosaccharides were
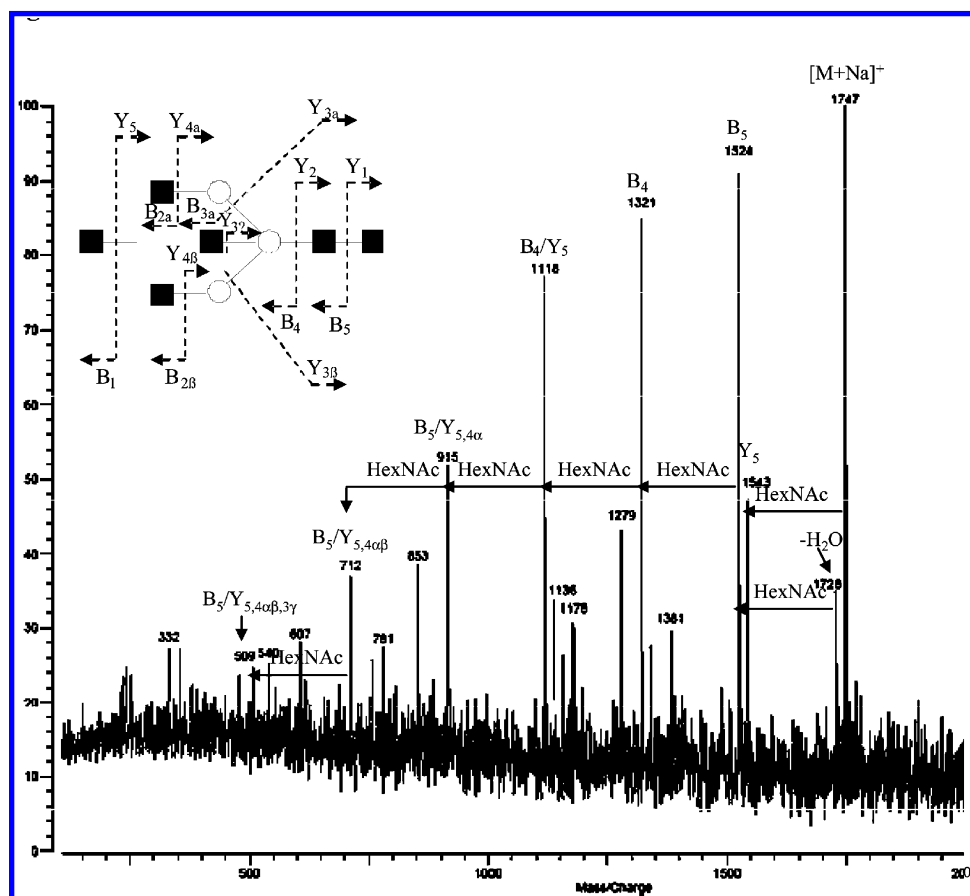
Figure 7. IRMPD spectrum of a glycan isolated from chicken ovalbumin (m/z 1746). No cross-ring cleavages are observed, but the rudimentary structure can be determined using the losses observed. The proposed structure is shown in the inset. The filled squares represent GlcNAcs, and the open circles represent mannoses.

examined. Two such oligosaccharides were obtained from bovine fetuin.

A monosialylated triantennary N-linked oligosaccharide was examined using MALDI. The IRMPD spectrum of the native N-linked glycan obtained from bovine fetuin is shown in Figure 5. The sodiated parent ion, m/z 2341 [M − H + 2Na]$^+$, was readily dissociated due to the facile loss of a sialic acid to yield the Y_6 ion (m/z 2027). This fragment ion further dissociates to produce essentially all other fragment ions. No fragment ions containing a sialic acid were observed.

Subsequent losses helped to elucidate the structure. These ions are combinations of reducing and nonreducing end fragments. For clarity, the combinations of losses are designated by "/" and include several series such as B_n and Y_n. For example, the B_6/Y_6 fragment comes from the loss of the sialic acid and the GlcNAc core. Other ions due to combination of cleavages include $B_6/Y_{6,5\alpha'}$ (m/z 1644), $B_6/Y_{6,4\alpha'}$ (m/z 1441), $B_6/Y_{6,4\alpha',5\alpha''}$ (m/z 1279), and $B_6/Y_{6,4\alpha',4\alpha''}$ (m/z 1076). These losses help define the connectivity of the glycan shown in the inset in Figure 5. A number of cross-ring cleavages at the reducing end are observed. These include $^{0,2}A_7/Y_6$, $^{2,4}A_7/Y_6$, and $^{2,4}A_6/Y_6$. Unlike the IRMPD of O-linked oligosaccharides, N-linked oligosaccharides yield a number of internal cross-ring cleavages. These cleavages ($^{0,2}A_5/Y_6$ and $^{2,4}A_6/Y_6$) correspond to the fragmentation at the branched points. These fragment ions are more evident in the examples to follow.

A trisialylated triantennary oligosaccharide was examined. The quasimolecular ion could not be obtained without methyl esteri-

fication of the sialic acids. The IRMPD of the methyl esterified ion is shown in Figure 6. Unlike the IRMPD of the native complex N-glycan (Figure 5) in which the sialic acid was readily lost, fragments containing the sialic acids were readily observed. For example, the B_6 (m/z 2722) ion corresponding to the loss of the reducing end GlcNAc is a prominent peak. The direct losses of methylated sialic acids were relatively minor peaks ($Y_{6\alpha'}$ at m/z 2638, $Y_{6\alpha',6\alpha''}$ at 2332). Sequential losses of sialic acids are observed, indicating the molecule is triply sialylated. Furthermore, the fragments containing $Y_{5\alpha'}$, $Y_{5\alpha''}$, and $Y_{5\beta}$ indicate that the sialic acids are located at the termini of each antenna. A number of cross-ring cleavages at the reducing end and branched points are observed. These include $^{2,4}A_7$, $^{0,2}A_7$, $^{0,2}A_7/Y_6$, $^{0,2}A_5$, and $^{2,5}A_6$.

Hybrid/Complex Core. A true hybrid oligosaccharide was not available for this investigation. Instead, the core structure of the hybrid/complex-type oligosaccharides was obtained by PNGase F release from ovalbumin. The resulting IRMPD spectrum of the native oligosaccharide is shown in Figure 7. This spectrum showed the quasimolecular ion at m/z 1746; however, the quality of the spectrum is poor because the amount of sample was severely limited. Nonetheless, there are significant fragment ions that provide some structural information. Unfortunately, the cross-ring cleavages are absent due to the low signal-to-noise ratio. A loss of H_2O is observed as a minor product, as with other oligosaccharides described previously. The major fragments are series corresponding to sequential losses of HexNAc. The loss of 203 from the quasimolecular ion means that the residue is from
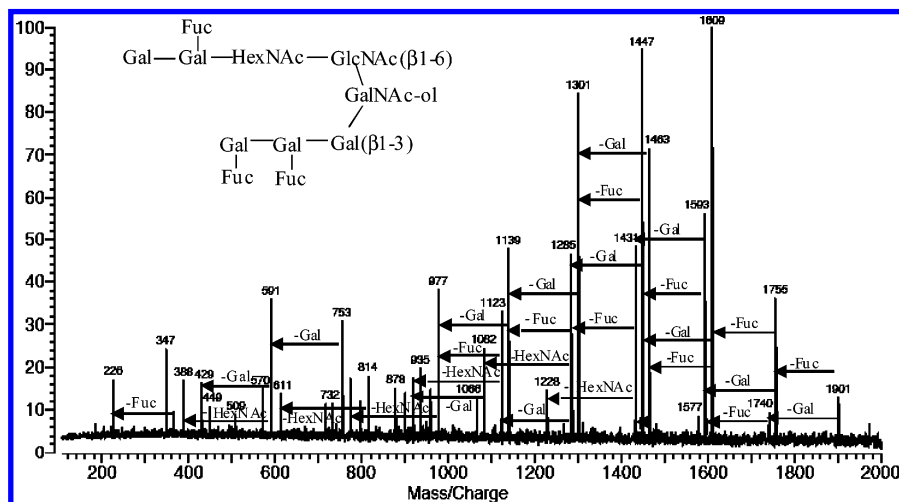
Figure 8. IRMPD spectrum of a large O-linked oligosaccharide isolated from *X. borealis* egg jelly coat (*m/z* 1901). This spectrum yields a large number of structural information, which allowed the determination of the preliminary structure (inset); however, no linkage information was obtained due to the lack of cross-ring cleavages.

the nonreducing end (Y_5). A loss of 221 (B_5) would indicate the loss of the reducing end. This product ion is accompanied by subsequent losses of other HexNAc residues from the nonreducing end. The resulting predicted structure is shown in the inset of Figure 7.

IRMPD of Large but Similarly Sized N- and O-Linked Oligosaccharides. A comparison of previous results on O-linked and the current N-linked oligosaccharides indicated major differences in the behavior of the two classes of compounds toward CID. O-Linked oligosaccharides are more amenable to fragmentation so that CID experiments often yielded good data.[23] However, CID of N-linked oligosaccharides yield fewer fragments, even for those with masses similar to those O-linked. In addition, N-linked oligosaccharides yielded internal cross-ring cleavages, but those O-linked never yielded cross-ring cleavages at the branch positions. To demonstrate that N-linked glycans fragment differently from O-linked glycans with IRMPD, two glycans with similar masses were compared. An oligosaccharide alditol from *X. borealis* egg jelly coat with a large molecular weight (*m/z* 1901) was isolated and fragmented using IRMPD. The resulting spectrum is shown in Figure 8. Clearly, no cross-ring cleavages were observed; however, rich structural information from the glycosidic bond fragmentation was obtained. These losses allowed for the determination of the preliminary structure (inset Figure 8) but no linkage information. For comparison, CID of *m/z* 1901 was performed (data not shown). CID required over five stages of tandem MS to obtain the final residue. At this point, the signal was lost, and no further sequence fragments were observed. The N-linked oligosaccharide that is comparable in molecular weight is Man 9 (*m/z* 1906, Figure 4). The N-linked IRMPD spectrum showed multiple cross-ring cleavages at the branching residues, none of which were observed for the O-linked oligosaccharide. The branching residues in N-linked oligosaccharides are often mannoses, but there are no mannose residues in O-linked oligosaccharides. Perhaps mannoses, when branched,

are more amenable to fragmentation than other branched saccharides.

CONCLUSIONS

The fragmentation observed in the CID and IRMPD spectra of N-linked oligosaccharides yields primarily glycosidic bond cleavages with cross-ring cleavages at the core branching mannoses. Cross-ring cleavages are important because they provide information regarding the linkages. Oligosaccharides often yield cross-ring cleavages at the reducing end, unless it is reduced to an alditol. Cross-ring cleavages are observed with both N- and O-linked oligosaccharides when high-energy CID conditions are used in a TOF/TOF instrument.[28] With several examples, Novotny and co-workers show extensive cross-ring cleavages representing fragmentation at nearly every residue. However, cross-ring cleavages of internal residues under low-energy CID conditions are not common. Cross-ring cleavages of internal residues do occur with N-linked oligosaccharides under both low-energy CID and IRMPD conditions, as shown here. Similar observations were reported by Harvey using a Q-TOF mass spectrometer.[29] In that work, cross-ring cleavages were observed also at the branching mannoses. Linear mannoses do not readily undergo the same fragmentation. Similarly, branch oligosaccharides that are not mannoses, such as those in O-linked oligosaccharides, do not readily produce the same cleavages. There is perhaps something stereochemically unique about a branched mannose that allows it to fragment in this way.

IRMPD has already been shown to be advantageous for the fragmentation of O-linked oligosaccharides, including sialyated and sulfated glycans.[20] This paper demonstrates that for N-linked sugars, IRMPD is still superior to low-energy CID for the determination of oligosaccharide structures.

(28) Mechref, Y.; Novotny, M. V.; Krishnan, C. *Anal. Chem.* **2003**, *75*, 4895–4903.

(29) Harvey, D. J. *J. Mass Spectrom.* **2000**, *35*, 1178–1190.